4 October 2002

Chemical Physics Letters 364 (2002) 237–243

CHEMICAL PHYSICS LETTERS

www.elsevier.com/locate/cplett

Photochemical induced effects in material ejection in laser ablation

Yaroslava G. Yingling, Barbara J. Garrison *

152 Davey Laboratory, Department of Chemistry, The Pennsylvania State University, University Park, Pennsylvania, PA 16802, USA

Received 11 May 2002; in final form 5 August 2002

Abstract

Molecular dynamics simulations are used to investigate the effect of photochemical processes on molecular ejection mechanisms in laser ablation of organic solids. The presence of photochemical decomposition processes and subsequent chemical reactions changes the temporal and spatial energy deposition profile from pure photothermal ablation. A strong and broad acoustic wave propagation results and this pressure wave in conjunction with the temperature increase in the absorbing region causes the ejection of hot massive molecular clusters. These massive clusters later disintegrate in the plume into the smaller clusters and monomers due to ongoing chemical reactions.

1. Introduction

Ultraviolet (UV) laser ablation has been extensively investigated because of the significance of its current and potential applications. Interaction of high power UV lasers with a substance typically results in the occurrence of photothermal and/or photochemical processes inside the material. Photothermal processes produce heat in the sample and photochemical processes exist where the UV photon energy is comparable with the chemical bond breaking energy. It is generally believed that in UV ablation these two processes are interrelated. The material ejection dynamic is dependent on the origin of the ablation process [1–4]. Due to the complexity of the processes involved in the chemical reactions, understanding the aspects of photochemistry in laser ablation is still a challenge.

The importance of photothermal and photochemical processes in laser ablation was examined in experiments where high concentration solutions (HCS) and low concentration solutions (LCS) of benzyl chloride in dichloromethane were compared [4]. It was noted that in HCS photochemical processes and in LCS photothermal processes were responsible for the onset of ablation. The photochemical regime was characterized by the presence of shock wave propagation with high initial velocity, dense gas-like plume and fast surface swelling. In addition, Tsuboi et al. [5] estimated the temperature of the surface region at the ablation threshold to be much lower than the boiling point of the material. In the case of the photo-

* Corresponding author. Fax: +1-814-863-5319.
E-mail address: bjg@chem.psu.edu (B.J. Garrison).

0009-2614/02/$ - see front matter
PII: S0009-2614(02)01327-1

thermal regime, the shockwave was not distinct and was observed only slightly at the early stage with low initial velocity and disappeared within a few milliseconds, a low plume density was detected and the surface swelling was delayed [6]. The LCS exhibited a much higher ablation threshold than HCS.

In our previous publication describing the incorporation of photochemical reactions in a mesoscopic breathing sphere molecular dynamics model of laser ablation [7], we reported that the presence of photochemical processes lowers the ablation threshold due to the release of additional energy from exothermic reactions into the irradiated sample and to the decrease of the average attractive bonding in the absorbing region. In this publication, we focus on the influence of photochemical processes on the material removal mechanism in the ablation regime. We compare the system with photochemistry to systems without photochemistry under thermal and stress confinement in the ablation regime [8]. The differences between thermal and stress confinement regimes for pure photothermal processes have been recently reported in detail in [8].

2. Computational setup

Our group has developed and applied a molecular dynamics model to study microscopic mechanisms of photothermal laser ablation [8–13]. The key aspect of this model is an approximate representation of internal atomic motions, which allows the expansion of the time and length scale of the system. Each molecule or group of atoms is represented by a single spherical particle. All particles are held together by pairwise additive intermolecular forces that describe the van der Waals interactions in a molecular solid. An internal degree of freedom, i.e. the breathing mode, is ascribed to each particle, allowing particles to change their sizes. Vibrational excitations are performed by depositing a quantum of energy equal to the photon energy into the kinetic energy of internal vibration of the excited molecules.

Recently, we have incorporated photochemical reactions into the breathing sphere model for irradiation conditions in which the photon energy exceeds the energy of the chemical bond [7,14]. The photochemical reaction of the excited molecule with the photon is represented by dividing the excited molecule into two radicals that can then react with other molecules in the system [7]. As a model system, the photofragmentation of the excited molecule and reactions of the fragments are based on the photochemistry of chlorobenzene. Chlorobenzene has been chosen because of the simplicity of its photofragmentation, entailing exclusively scission of the C–Cl bond to yield C_6H_5 and Cl radicals, and the availability of extensive experimental data [5,15–19]. The chlorine and phenyl radicals can react with the chlorobenzene or other radicals by various abstraction and radical–radical recombination reactions, yielding various products such as HCl, Cl_2, C_6H_6, $C_6H_4Cl_2$, $C_{12}H_{10}$, $C_{12}H_8Cl_2$ and $C_{12}H_9Cl$. A complete description of the computational setup, the potential parameters, and the list of reactions along with their exothermicities are given in [7]. The probability of occurrence of the various reactions depends on the distance between the reactants and the temperature of surroundings. The heat of reaction is used to determine the change in potential and kinetic energy of the reaction products and their surroundings. The deposition of the energy is carefully monitored throughout the calculations. The absorption of a UV photon is not allowed in the photoproducts.

The laser irradiation at 248-nm wavelength is simulated by photochemical or vibrational excitation of random molecules during the 15 or 150 ps laser pulse within a 50 nm penetration depth. The attenuation of the laser light with depth follows Beer's law. The percentage of the excited molecules to undergo photofragmentation can be varied. The simulation is performed on a sample with 130 000 molecules ($10\ \text{nm} \times 10\ \text{nm} \times 191\ \text{nm}$). Periodic boundary conditions are imposed in the directions parallel to the surface. At the bottom of the sample, the non-reflecting dynamic boundary conditions are applied in order to avoid artificial effects due to pressure reflection [20].

Three simulations were performed at a fluence of 40 J/m^2, a value above the ablation threshold for all the simulations. The first two systems have

only vibrational excitation due to the laser irradiation and are for pulse widths of 150 or 15 ps so that the system is in thermal or stress confinement, respectively [8]. The last simulation has a 150 ps laser pulse, but assumes that 36% of the excited molecules undergo photochemical fragmentation and 64% of excited molecules undergo vibrational excitation. This specific percentage has been observed experimentally for 248-nm laser photodecomposition of a beam of chlorobenzene molecules [17]. An inference of the quantum yield of bond scissions has been made in experiments of the laser ablation of chlorobenzene molecular films, in which the photodissociation yield of 5% was estimated from the fraction of HCl molecules in the plume [16]. Our simulations with 5% photofragmentation predict less than 2% of the HCl molecules in the plume [7]. On the other hand, our simulation with 36% photofragmentation exhibits a 5% concentration of HCl molecules in the plume.

3. Results and discussion

The addition of photochemistry to the ablation process alters the energy deposition events both temporally and spatially from the pure photothermal irradiation. This change in energy deposition has direct consequences on the pressure and temperature developed in the system which then influence the plume characteristics. First, the difference of the enthalpy deposition profiles due to the presence of photochemical reactions is examined. Second, the influence of the energy deposition on the pressure wave profiles is shown. Last, the differences in the plume composition and density are discussed.

The photochemistry involved with bond scission and subsequent chemical reactions means that the energy available for ablation processes is not simply the laser fluence [7]. The temporal profiles of total enthalpy deposited per picosecond in the sample are plotted for the 40 J/m^2 laser fluence for the three simulations in Fig. 1a. In the absence of photochemistry, the enthalpy deposited in the sample depends on the number of photons absorbed per picosecond where each 248 nm photon

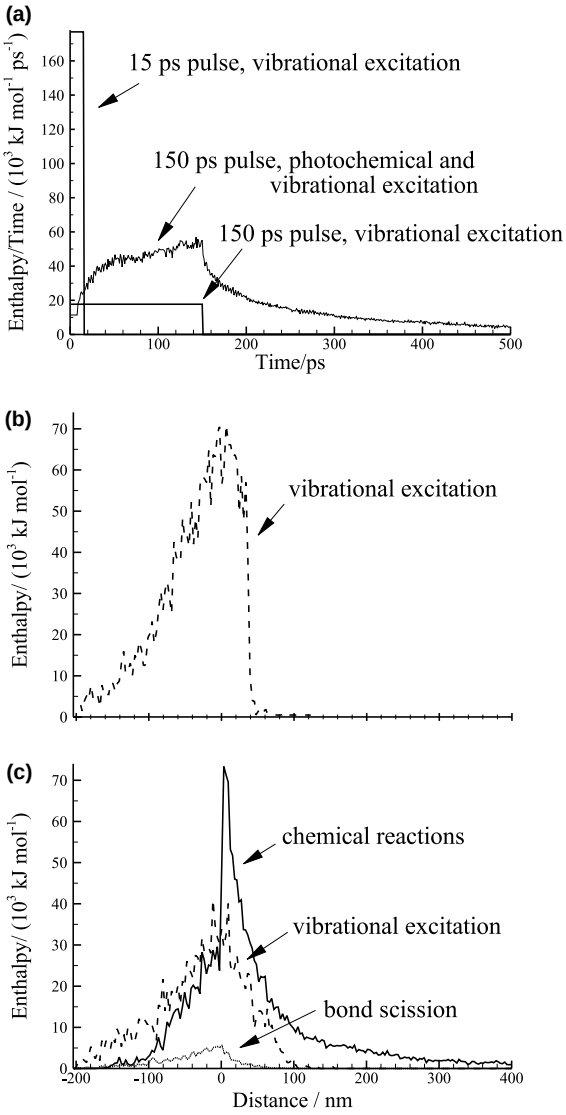

Fig. 1. Enthalpy deposited in the sample. (a) Enthalpy deposited per picosecond vs. time for three different simulation conditions. (b) Enthalpy deposited vs. distance integrated over time for vibrational excitation energy deposition. The surface was initially at a distance of 0 nm. (c) Enthalpy deposited vs. distance integrated over time for mixed photochemical and photothermal energy deposition.

converts to 482 kJ/mol. The situation is completely different, however, when the photochemical processes are present in the sample. In this case, 36% of the excited molecules break up into the fragments, where the majority of the photon energy is

spent on scission of the chemical bond. The available energy for the photoproducts is about 72 kJ/mol [17]. Therefore, at the beginning of the laser pulse the deposited enthalpy in this system is lower than in the case with only photothermal processes. During these first 10 ps the amount of reactive photofragments accumulates in the sample and the temperature rises thus increasing the mobility of the photofragments and increasing the probability that reactions occur. After about 10 ps the fragments begin to react via radical–radical recombination and via abstraction reactions with the parent molecule [7]. These reactions are exothermic and release an additional enthalpy, ranging from 30 up to 500 kJ/mol, into the system. Although the laser fluences for the photothermal and photochemical simulations are identical, the exothermic reactions in the photochemical simulation provide more energy that is available for translational motions of the particles.

The time integrated spatial distribution of the deposited enthalpy is also different between the photothermal and photochemical systems as shown in Figs. 1b, c. For the system with only vibration excitation, the enthalpy deposition originates completely from the laser irradiation and follows Beer's law as shown in Fig. 1b. Since the surface expands or swells slightly during the laser pulse, some of the energy is deposited at distances of 0–40 nm. The small enthalpy increase at distances from 50 to 100 nm is absorption by gas phase species. The spatial enthalpy deposition profile for the photochemical system is more complex as shown in Fig. 1c. The vibrational excitation and the bond scission contributions exhibit the Beer's law absorption profile. The enthalpy increase due to the chemical reactions, however, reflects the temperature in the system. The temperature is hottest near the surface of the system thus the enthalpy increase is greatest there. The increase in enthalpy due to chemical reactions does not penetrate as far into the surface (negative distances) as the enthalpy increases due to vibration excitation. Moreover, there are numerous reactions in the gas phase of the ablated plume. The chemical reactions provide an additional energy into the overheating of the system and the ablation event as well as increase the energy of the plume. Comparison of Figs. 1b, c shows that the surface swells more and, in fact, faster with photochemical processes than with only photothermal processes, an observation confirmed by experimental results [4,5].

The rate of enthalpy deposition in the photochemical system is between that of the thermal and stress confinement regimes, thus the pressure development should be intermediate too. The temporal pressure wave profiles are calculated for the three simulations at 100 nm under the surface and are shown in Fig. 2. As discussed in [8], in the case of stress confinement (15 ps pulse) the pressure wave is very strong and sharp. For the vibrational excitation system under thermal confinement (150 ps pulse) the pressure wave is not as intense and is much broader. As suggested by the enthalpy deposition profiles shown in Fig. 1, the pressure wave is about three times stronger for the system with photochemistry than for the vibrational excitation system under thermal confinement, but more spread out than in the system under stress confinement. This observation agrees with the experimental observation that photochemical ablation is usually characterized by the presence of shock wave propagation with a high initial velocity [4,5], whereas in the photothermal regime the shock-wave was not distinct and was observed only slightly at an early stage with low initial velocity, disappearing within few microseconds [4,6].

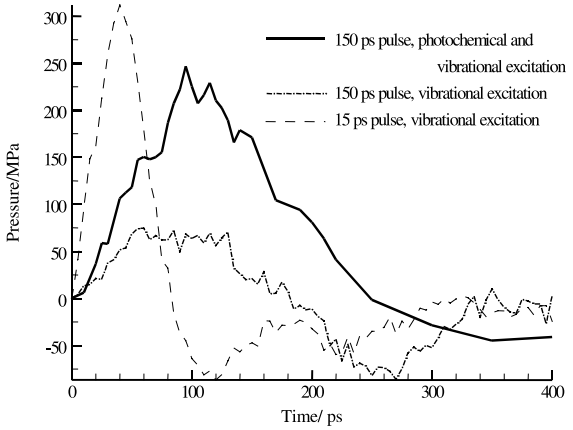

Fig. 2. Temporal pressure profiles at 100 nm below the surface. Positive pressure is related to compressive stress and negative pressure to tensile stress.

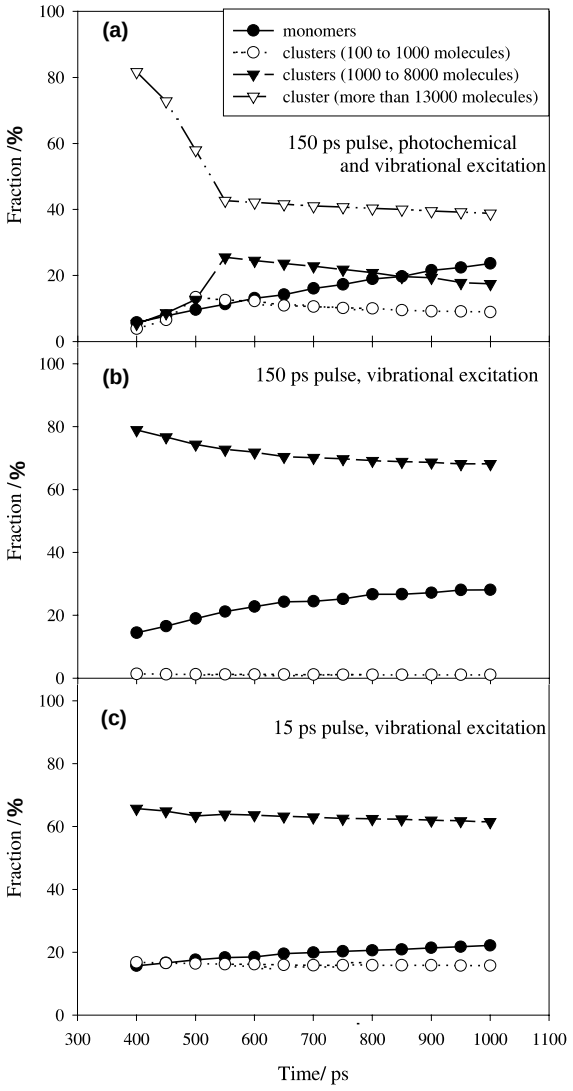

Fig. 3. Plume composition vs. time.

The strong pressure in the photochemical system (Fig. 2) coupled with the exothermic reactions that continue beyond the pulse (Fig. 1a) and into the plume (Fig. 2c) suggests that clusters ablated may be larger and hotter than for pure vibrational excitation [8]. The change in cluster sizes is shown in Fig. 3 for the three simulations. The average flow velocity in the axial direction at 1 ns are given in Table 1. Finally, the density of the plume at 1 ns is shown in Fig. 4. Peaks in the density plot correspond to individual clusters and the monomer intensity is given by the background-like intensity. Below we briefly describe the characteristics of the ablation plumes in thermal and stress confinement to put in perspective the plume conditions with photochemistry. A full discussion of the plumes with vibrational excitation is given in [8].

Thermal confinement in which ablation is caused by an explosive boiling phase transition is characterized by ejected clusters that are relatively hot as indicated in Fig. 3b with the larger clusters decreasing in size as time progresses and the number of monomers increasing in time. The plume consists primarily of larger clusters (>1000 molecules) and individual molecules or monomers. The temperature of the clusters is reflected by the low density of the cluster peaks in Fig. 4b. On average, the monomer density is less than $\sim$0.01 g/cm^3.

Stress confinement, where the laser-induced pressure contributes to the prompt material ejection, is characterized by relatively cold clusters as indicated by the slower decline in intensity of the clusters with time as shown in Fig. 3c. There are also three peaks in Fig. 4c in which the density is greater than 0.8 g/cm^3, i.e., nearly as dense as the original material and there are relatively dense clusters that exist at distances of almost a micron above the surface. The interaction of strong pressure wave with material result in many more clusters in the intermediate size (100–1000 particles) as shown in Fig. 3c than explosive boiling. The background density of monomers is negligible

Table 1
The axial velocities in m/s for the monomers and clusters in the plume at 1 ns

	Monomers	Clusters of more than 1000 molecules
Photochemical and vibrational excitation, 150 ps pulse	720	102
Vibrational excitation, 150 ps pulse	490	69
Vibrational excitation, 15 ps pulse	629	245

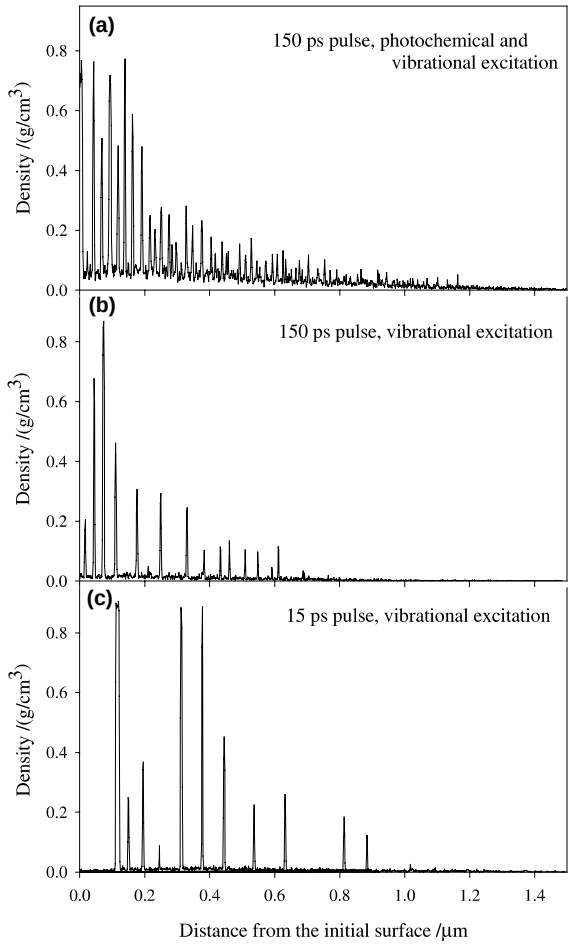

Fig. 4. Density of the plume vs. the distance from the initial surface at 1 ns simulation time.

because as shown in Table 1, the monomers have very high velocities and spread out. The high pressure pushes both the monomers and clusters from the surface with greater axial velocities as shown in Table 1 and by the extent of the plume in Fig. 4c than the explosive boiling of thermal confinement.

Photochemically driven ablation, on the other hand, causes massive molecular clusters ranging from 15 000 to 35 000 molecules to ablate as shown in Fig. 3a. Since the reactions continue to proceed in the plume and after the laser pulse as shown in Fig. 1, the large clusters rapidly disintegrate until about 500 ps when the chemical reactions cease. After this time, the molecules escape from the clusters mainly due to evaporation. Even at 1 ns, approximately 40% of the plume is in clusters of more than 13 000 molecules. There are many more medium-sized individual clusters that correspond to densities up to 0.3 g/cm^3 at large distances from the surface as shown by the peaks in Fig. 4a than for either thermal or stress confinement. The big clusters are closest to the surface. On average at 1 ns the clusters are still liquid and will continue to evaporate. The monomer intensity is approximately 0.05 g/cm^3, considerably higher than either thermal or stress confinement. The axial velocity of the monomers (Table 1) is greater than in stress confinement but the axial velocity of the clusters is relatively low. The dense gas-like plume was observed by experiment in the system where ablation was triggered by photochemical processes [4,5].

4. Conclusions

The comparison between simulations with different rates of enthalpy deposition shows that the system with the presence of photochemical processes exhibits a different mechanism of molecular ejection. The photochemical fragmentation and the consequent chemical reactions create a local pressure build up and generate a strong pressure wave. The strong pressure wave and increase of the temperature in the absorbing region are responsible for the ejection of big molecular clusters. The ejected clusters disintegrate into smaller clusters and monomers later on due to ongoing chemical reactions. The ejection and disintegration of big clusters result in the higher material removal rates and plume density. These results are in good agreement with experimental observations, where the presence of photochemistry was attributed to the strong pressure wave propagation and high plume density [4,5].

Acknowledgements

This work is supported by Air Force Office of Scientific Research through the Medical Free Electron Laser Program, Multidisciplinary University Research Initiative, and Chemistry Divi-

sion of the National Science Foundation. The computational support was provided by the Center for Academic Computing at Penn State University. We thank Leonid Zhigilei for helpful discussions and reading the manuscript.

References

[1] R. Srinivasan, Science 234 (1986) 559.
[2] R. Srinivasan, A.P. Ghosh, Chem. Phys. Lett. 143 (1988) 546.
[3] M. Buck, P. Hess, Appl. Surf. Sci. 43 (1989) 358.
[4] K. Hatanaka, M. Kawao, Y. Tsuboi, H. Fukumura, J. Appl. Phys. 82 (1997) 5799.
[5] Y. Tsuboi, K. Hatanaka, H. Fukumura, H. Masuhara, J. Phys. Chem. 98 (1994) 11237.
[6] Y. Tsuboi, H. Fukumura, H. Masuhara, J. Phys. Chem. 99 (1995) 10305.
[7] Y.G. Yingling, L.V. Zhigilei, B.J. Garrison, J. Photochem. Photobiol. A 145 (2001) 173.
[8] L.V. Zhigilei, B.J. Garrison, J. Appl. Phys. 88 (2000) 1281.
[9] L.V. Zhigilei, P.B.S. Kodali, B.J. Garrison, J. Phys. Chem. B 101 (1997) 2028.
[10] L.V. Zhigilei, P.B.S. Kodali, B.J. Garrison, J. Phys. Chem. B 102 (1998) 2845.
[11] L.V. Zhigilei, P.B.S. Kodali, B.J. Garrison, Chem. Phys. Lett. 276 (1997) 269.
[12] L.V. Zhigilei, B.J. Garrison, Appl. Phys. Lett. 74 (1999) 1341.
[13] L.V. Zhigilei, Y.G. Yingling, T.E. Itina, T.A. Schoolcraft, B.J. Garrison, Int. J. Mass Spectrom. Franz Hillenkamp, special issue, in press.
[14] Y.G. Yingling, L.V. Zhigilei, B.J. Garrison, Nucl. Instrum. Methods Phys. Res. B 180 (2001) 171.
[15] Y. Tsuboi, K. Hatanaka, H. Fukumura, H. Masuhara, J. Phys. Chem. A 102 (1998) 1661.
[16] S. Georgiou, A. Koubenakis, M. Syrrou, P. Kontoleta, Chem. Phys. Lett. 270 (1997) 491.
[17] S. Georgiou, A. Koubenakis, J. Labrakis, M. Lassithiotaki, J. Chem. Phys. 109 (1998) 8591.
[18] S. Georgiou, A. Koubenakis, J. Labrakis, M. Lassithiotaki, Appl. Surf. Sci. 127 (1998) 122.
[19] T. Ichimura, Y. Mori, H. Shinohara, N. Nishi, Chem. Phys. 189 (1994) 117.
[20] L.V. Zhigilei, B.J. Garrison, Mater. Res. Soc. Symp. Proc. 538 (1999) 491.